

Structure constrained least-squares migration of total reflection and its applications

Cheng Cheng*, Yang He, Jian Mao, Bin Wang (TGS)

Introduction

Least-squares imaging of primary reflection can overcome acquisition limitations and recover the reflectivity for desired amplitudes and resolutions (Wang et al., 2013). In shallow water environment, migration of multiples can help improving image quality at water bottom and shallow structure since it broadens the illumination compare to primary. But it also can suffer from strong crosstalk among multiples as well as diminished deep structure for lack of recorded surface multiple energy. Iterative data-domain least-squares migration of total reflection (LSMTR) gets benefit from both primary and all orders of multiple signals available in the data. More beneficially, it also can effectively suppress the crosstalk by iteratively data subtraction and remigration as well as an inversion-based deconvolution imaging condition. It produces a crosstalk free image with balanced contribution from each component including primary and multiples.

The proposed LSMTR estimates the reflectivity model by finding the best least-squares fit of the modeled data to the observed data, using a gradient-based iterative method. However, one cannot match all the complex features present in field data with only a linearized Born modeling operator. Without any constraint on the inversion gradient, the noise content will also increase with iterations. This increased noise mostly arises from velocity model error, a wider bandwidth of pre-existing linear noise in the data and back scattered energy due to the presence of strong contrasts in the velocity model (Wang et al., 2016). Regularization or preconditioning can be applied in iterative algorithm to suppress migration artifacts, speed up convergence and improve inversion efficiency. In addition, proper fault constraints can not only preserve the real geological features but also improve the efficiency of inversion.

In this work, we propose to utilize total reflection wavefield in a least-square sense and use convolutional neural networks (CNNs) to automatically detect faults as a structure constraint during inversion. Two field examples are shown here to demonstrate the capability of the algorithm.

Methodology

Least-squares migration of total reflection

In conventional least-squares primary migration, a point source is used and the upgoing deghosted and demultiplied primary wavefield acts as the boundary observation for inversion. In LSMTR, the deghosted total downgoing wavefield consisting of both primaries and multiples is included in the source wavefield, and the total upgoing wavefield

consisting of both primaries and multiples acts as full wavefield data for inversion. Since the inverted full wavefield image contains contribution from both primary and multiple reflected energy simultaneously, it can improve images in comparison to standard migration using only primary or multiple. And the inversion helps with reducing the strong crosstalk produced by interference between different orders of reflections. However, for tower stream data, it is challenging to balance the contribution between point source and downgoing wavefield. We adopt the approach as in Tu et al. (2016) to invert for another parameter λ which represents the point source amplitude estimation during the inversion.

Preconditioning with deep learning based structure constraint

The objective function of preconditioned LSMTR can be expressed as:

$$f(\bar{m}) = \min_{\bar{m}} \|\bar{d} - A[\lambda s - \bar{d}]S^{-1}S\bar{m}\|^2$$

where $f(\bar{m})$ stands for the cost function to be minimized, $A[\lambda s - \bar{d}]$ is the linearized Born modeling operator which is the exact adjoint of the migration operator and S is a preconditioning operator. In this study, acoustic one-way wave-equation operators are used.

We adopt structure-oriented smoothing with edge-preservation as preconditioning (Hale, 2009) in LSMTR to suppress migration artifacts caused by irregular sampling or overfitting to the data noise:

$$g'(\bar{x}) - \frac{\sigma}{2} \nabla \cdot D(\bar{x}) \cdot \nabla g'(\bar{x}) = g(\bar{x})$$

while $D(\bar{x})$ is tensor-valued filter coefficients, $g(\bar{x})$ is the raw gradient and $g'(\bar{x})$ is the structure smoothed gradient. The tensors $D(\bar{x})$ can be scaled by any measure of coherence that is almost zero near discontinuities and approximately one where features are most coherent to preserve edges during smoothing. We calculate the semblance based on structural tensors which is imposed as a smoothing weight. This allows us to use machine picked fault likelihood as an additional constraint during inversion.

Machine learning is becoming more useful in seismic interpretation, with one of its most successful applications being fault picking on seismic images. Most recently, some CNN methods have been introduced to detect faults by pixel-wise fault classification (fault or non-fault) with multiple seismic attributes (Wu et al., 2019). Here we use similar approach in that paper which considers fault detection as an

Structure constrained least squares migration of total reflection and its field applications

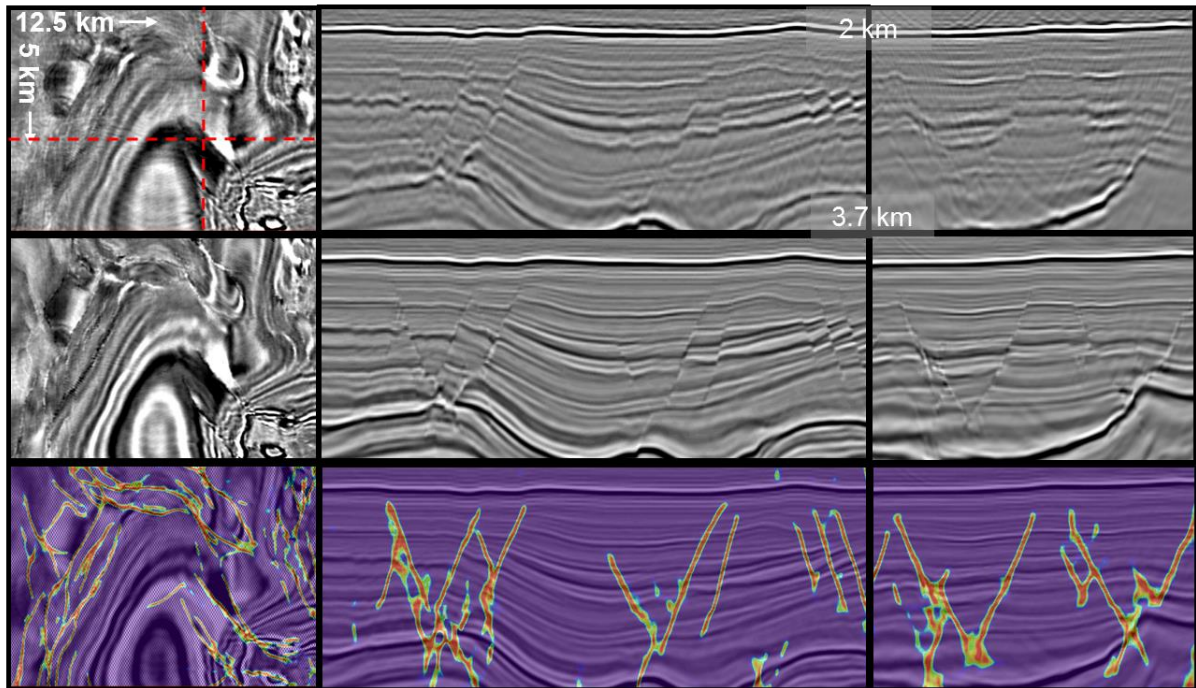


Figure 1: Santos Basin field data examples: The top row is the conventional migration; the middle row shows the final structure-constrained least-squares migration image at 5th iteration; the bottom row shows machine-picked fault probability. Left column figures show map view while middle column shows inline view and right column shows crossline view. The inline and crossline positions are indicated on first figure.

efficient end-to-end binary image segmentation problem using CNNs. It generates accurate fault likelihood maps on real datasets using multiple powerful CNN architectures to obtain superior segmentation results. We train our CNN model in two steps. First, we repeat the procedure of Wu et al. by training and validating with 200 and 20 pairs of synthetic seismic and fault images with only random noise added on, respectively. The resulting CNN model cannot distinguish between faults and migration swings on a field dataset which is heavily contaminated by migration swings. Since Tensorflow and Keras allow for continued training based on a pre-loaded model, we next added migration swings to each synthetic image. Starting from the previous pretrained CNN model we continue the training process until the training and validation accuracy converges. The CNN model we obtain from this second training step performs better than the pretrained model in distinguishing faults from migration swings, for both synthetic and real datasets.

Field data examples

NAZ dataset from Santos Basin

First, we demonstrate our preconditioned least-squares migration using a field data example in Santos Basin,

offshore Brazil. This is a narrow azimuth dataset (NAZ), acquired with 10 cables, 100 m streamer separation and 8 km streamer length. The sedimentary images in this area suffer from uneven illumination, visible migration artifacts, and sub-optimal resolution.

As shown in Figures 1, our deep learning structure-constrained least-squares technique helps resolve these problems, and the final image is better suited to reservoir characterization. The middle and right columns of Figure 1 show the comparison between the final least-squares image and conventional migration in inline and crossline directions. With automatic machine-picked fault probability (last row in Fig. 1) imposed as the smooth weighting, the final result shows the benefits of conventional least-squares imaging without boosting overfitting noise. Compared with conventional smoothing preconditioning, our algorithm results in higher lateral resolution and sharper dipping fault planes in the sediment layer. Left column of Figure 1 shows the depth slice comparison at around 2.8 km in the same volume. It clearly indicates an enhancement in imaging the fault planes and improving spatial resolution.

Structure constrained least squares migration of total reflection and its field applications

WAZ dataset from Declaration

Second, we further demonstrate our structure constraint LSMTR in extremely shallow water environment by showing another inline result in Declaration project. This is a tower streamer wide azimuth dataset (WAZ). The input data underwent a typical processing flow involving denoise, deghost, and velocity model building steps. The image area

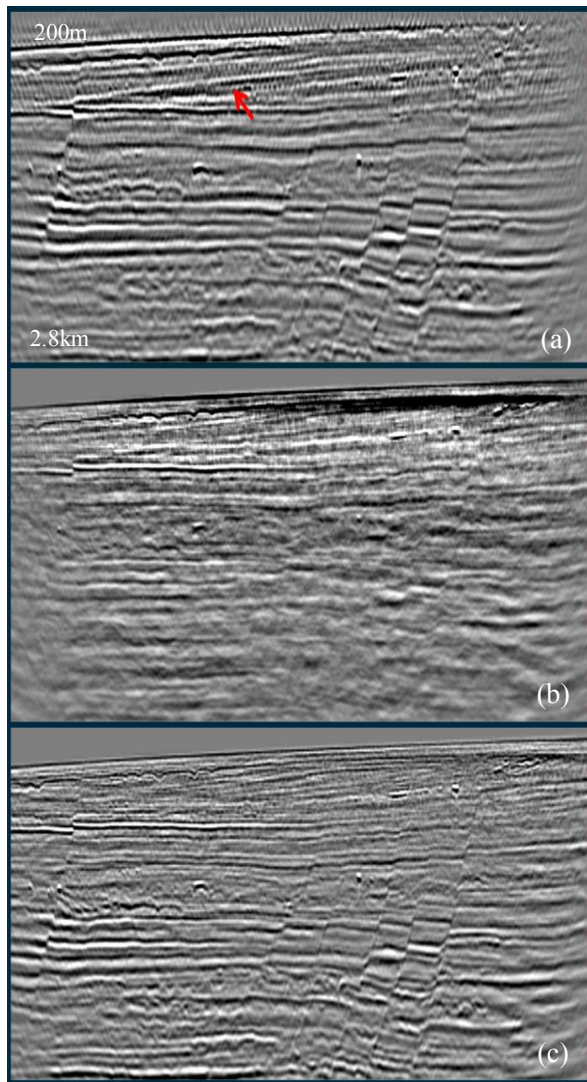


Figure 2: Inline image for Declaration field data examples: (a) conventional primary only migration, (b) conventional multiple only migration, (c) LSMTR with structural constraint at 4th iteration.

we cropped has a water bottom ranges only 200~300m. Fig.

2a shows results of the conventional primary migration. It shows unbalanced illumination, especially for the shallow structure which is contaminated by strong acquisition footprint. Besides, the interference of all-orders of data generates strong crosstalk in the hard, shallow water bottom environment. Fig. 2b shows the conventional multiple migration. It partly solves the problem by better illumination in the shallow. But again, the crosstalk issue still exists and the deep structure is under poor illumination and buried by interference noises. Fig. 2c shows the final solution provided by our LSMTR technique. It solves all the issues in conventional imaging by balanced illumination from all orders of data, reduced crosstalk noise and with wider frequency-wavenumber band. Especially to the upper right where the water bottom depth is reaching 200m, the shallow structure and water bottom itself stands out quite clear. Specifically, the red arrow in Fig. 2a which indicates a multiple crosstalk is removed. Besides the faults structure is enhanced by preconditioning, more coherent seismic events and less migration noise shows in the final solution.

Conclusion

With advanced structure-constrained LSMTR algorithm, improved imaging of shallow water sedimentary geometries, minimized migration artifacts, significantly increased image resolution and enhanced fault structure can be achieved in few iterations. The final least-squares image with Santos Basin and LSMTR images with Declaration field dataset demonstrate our claim. Modern advanced imaging techniques like FWI and least-squares are required to run within limited production time for high quality large-scale multi-client projects. With help from machine learning, our highly efficient and automated LSMTR technique makes it feasible.

Acknowledgements

The authors would like to thank TGS management for permission to publish this paper.

REFERENCES

- Hale, D., 2009, Structure-oriented smoothing and semblance: CWP Report, 635.
- Tu, N., A. Y. Aravkin, T. van Leeuwen, T. T. Lin, and F. J. Herrmann, 2016, Source estimation with surface-related multiples — Fast ambiguity-resolved seismic imaging: *Geophysical Journal International*, **205**, 1492–1511, doi: <https://doi.org/10.1093/gji/ggw097>
- Wang, B., S. Dong, and S. Suh, 2013, Practical aspects of least-squares reverse time migration: 75th Conference and Exhibition, EAGE, Extended Abstracts, <https://doi.org/0.3997/2214-4609.20131000>.
- Wang, P., A. Gomes, Z. Zhang, and M. Wang, 2016, Least-squares RTM: reality and possibilities for subsalt imaging: 86th Annual International Meeting, SEG, Expanded Abstracts, 4204–4209, doi: <https://doi.org/10.1190/segam2016-13867926.1>.
- Wu, X., 2017, Directional structure-tensor based coherence to detect seismic faults and channels: *Geophysics*, **82**, no. 2, A13–A17, doi: <https://doi.org/10.1190/geo2016-0473.1>
- Wu, X., L. Liang, Y. Shi, S. Fomel, 2019, FaultSeg3D: using synthetic datasets to train an end-to-end convolutional neural network for 3D seismic fault segmentation: *Geophysics*, K1–K9, doi: <https://doi.org/10.1190/geo2018-0120.1>.